

Bonding in Low-Coordinate Environments: Electronic Structure of Pseudotetrahedral Iron–Imido Complexes

Espen Tangen,[†] Jeanet Conradie,^{†,‡} and Abhik Ghosh^{*,†}

Center for Theoretical and Computational Chemistry, Department of Chemistry, University of Tromsø, N-9037 Tromsø, Norway, and Department of Chemistry, University of the Free State, 9300 Bloemfontein, Republic of South Africa

Received November 6, 2006

Abstract: A detailed density functional theory study of pseudotetrahedral Fe^{III/IV}–imido–phosphine complexes has yielded a host of new insights. The calculations confirm $d_{xy}^2d_{x^2-y^2}d_{z^2}^1$ (or $d_{\delta}^2d_{\delta'}^2d_{\sigma}^1$) electronic configurations for Fe^{III}–imido complexes of this type, as previously proposed, where the z direction may be identified with the Fe–N_{imido} vector. However, geometry optimization of a sterically unencumbered model complex indicated a bent (162°) imido linkage, in sharp contrast to the linear imido groups present in the sterically hindered complexes that have been studied experimentally. Under C_{3v} symmetry, the Fe^{III}–imido molecular orbital (MO) energy-level diagram indicates the existence of near-degenerate 2A_1 and 2E states, and accordingly, the bending of the imido group appears to be ascribable to a pseudo-Jahn–Teller distortion. For Fe^{IV}–imido complexes, our calculations indicate a $d_{xy}^2d_{x^2-y^2}^1d_{z^2}^1$ (or $d_{\delta}^2d_{\delta'}^1d_{\sigma}^1$) electronic configuration, which is somewhat different from the $d_{xy}^1d_{x^2-y^2}^1d_{z^2}^2$ (or $d_{\delta}^1d_{\delta'}^1d_{\sigma}^2$) configuration proposed in the literature. Not surprisingly, for a sterically unencumbered Fe^{IV}–imido complex, the degenerate 3E state (under C_{3v} symmetry) results in a mild Jahn–Teller distortion and a slightly bent (173°) imido linkage (on relaxing the symmetry constraint). The calculations also shed light on the surprising stability of the d_{z^2} -based MO, which points directly at the imido nitrogen, relative to the d_{π} -based MOs. The low-coordinate nature of the complexes—the absence of equatorial ligands and of a ligand trans with respect to the imido ligand—plays a key role in stabilizing the d_{z^2} orbital as well as the complexes as a whole. The electronic configurations of Fe^{IV}–imido porphyrins are radically different from that of the pseudotetrahedral complexes studied here, and we have speculated that these differences may well account for the nonobservation so far of Fe^{IV}–imido porphyrins.

The vast majority of oxo^{1,2} and imido^{3,4} complexes synthesized to date involve early transition metals with d^0 , d^1 (d_{δ}^1), or d^2 (d_{δ}^2) electronic configurations. It has long been appreciated that the stability of these complexes owes largely to the absence of antibonding d_{π} – p_{π} interactions.^{5,6} By the same logic, multiply bonded metal–ligand units in

volving middle and late transition metals are not expected to be stable. Thus, Fe^{IV}O,^{7,8} Mn^{IV}O,^{9,10} and Fe^VN^{11,12} porphyrins as well as Fe^{VO} corroles^{13,14} are all highly reactive species, while Fe^{IV}–imido porphyrins¹⁵ remain unknown. In recent months and years, however, a handful of low-coordinate, late transition metal imido complexes have been synthesized and even crystallographically characterized.⁴ By and large, high-quality density functional theory (DFT) calculations have accompanied these synthetic studies.⁴ Interestingly, the calculations indicate that, although these complexes exhibit a strong tendency to avoid occupancy of

* Corresponding author fax: +47 77644065; e-mail: abhik@chem.uit.no.

[†] University of Tromsø.

[‡] University of the Free State.

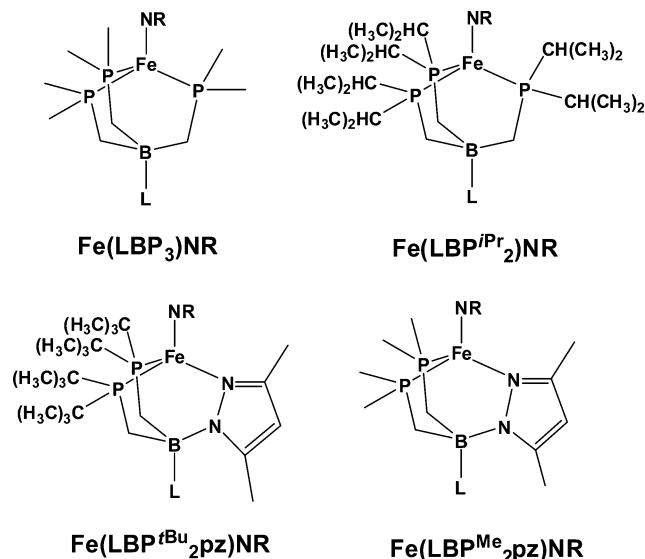


Figure 1. Different ligands considered in this study, depicted as their Fe=NR complexes. R = Me or Ad, L = Me or Ph.

the d_{π} – p_{π} antibonding orbitals, a d_{σ} orbital, pointing directly at the imido nitrogen, is invariably occupied, either singly or doubly, in all of these complexes.⁴ To understand the unexpected stability of this metal(d_{σ})–N_{imido}(p_{σ}) antibonding orbital, we have undertaken a DFT survey of the various known classes of transition-metal–imido complexes. In this paper, we present the results of an aspect of our studies that has been brought to a certain conclusion, namely, an account of Fe^{III/IV}–imido bonding in pseudotetrahedral complexes with phosphinoborate supporting ligands.^{16–19}

Figure 1 depicts the various supporting ligands used either experimentally or in our calculations. For the low-spin $S = 1/2$ Fe^{III}–imido complex Fe^{III}(PhBP^{iPr}₃)(NAd),¹⁸ which has a near-linear Fe–N_{imido}–C unit, DFT calculations indicated a $d_{xy}^2d_{x^2-y^2}^2d_{z^2}^1$ (or $d_{\delta}^2d_{\delta'}^2d_{\sigma}^1$) electronic configuration. The literature is relatively silent on why the d_{z^2} orbital, which points directly at the strongly σ -donating imido ligand, starts to fill ahead of the Fe d_{π} orbitals. Similarly, a $d_{xy}^1d_{x^2-y^2}^1d_{z^2}^2$ (or $d_{\delta}^1d_{\delta'}^1d_{\sigma}^2$) electronic configuration has been proposed for the $S = 1$ Fe^{IV}–imido complex [Fe^{IV}(PhBP^{tBu}₂pz)(NAd)]⁺.¹⁹ Although we will see that DFT calculations indicate a somewhat different $d_{\delta}^2d_{\delta'}^2d_{\sigma}^1$ configuration for this complex, the question still remains why the d_{z^2} orbital fills before the d_{π} orbitals. In the same vein, all known pseudotetrahedral Co^{III}–imido complexes exhibit $S = 0$ $d_{xy}^2d_{x^2-y^2}^2d_{z^2}^2$ (or $d_{\delta}^2d_{\delta'}^2d_{\sigma}^2$) ground states,^{20,21} although in one case, an $S = 1$ $d_{xy}^2d_{x^2-y^2}^2d_{z^2}^1d_{xz}^1$ (or $d_{\delta}^2d_{\delta'}^2d_{\sigma}^1d_{\pi}^1$) excited state is thermally accessible above room temperature.^{22,23} Similarly, a β -diketiminato–Co^{III}–imido complex also exhibits an $S = 0$ ground state, indicating nonoccupancy of the two d_{π} orbitals.²⁴ This, then, is the central question we sought to clarify in this study: what accounts for curious stability of the metal d_{z^2} orbital in these complexes, relative to the d_{π} orbitals?

Methods

All calculations were carried out using the VWN local density functional, the PW91²⁵ generalized gradient approximations (GGA) for both exchange and correlation, triple- ζ plus polarization Slater-type orbital basis sets, and a fine mesh for the numerical integration of matrix elements, as implemented in the ADF 2005²⁶ program system. As a check on the performance of the PW91 functional, the OLYP²⁷ GGA was also used for several calculations. In general, the PW91 GGA favors a distinctly more covalent, spin-paired description for transition-metal–ligand interactions, compared to OLYP.^{28,29} In this study, however, both GGAs yield very similar results (geometries, spin densities, and energetics). Moreover, we did not encounter any warning signs such as unexpected bond distances or spin density profiles that might have indicated that DFT might not be a suitable approach for this study.^{28,29} Accordingly, in this initial study, we have not felt the need to deploy multiconfigurational ab initio methods.^{30,31}

Results

(a) Fe^{III}–Imido Trisphosphine Complexes. Figure 2 depicts various calculated results on the simplified, sterically unencumbered C_{3v} Fe^{III}(MeBP₃)(NMe) complex, while Figure 3 presents analogous results from symmetry-unconstrained optimizations of Fe^{III}(PhBP^{iPr}₃)(NAd), the actual molecule studied experimentally.¹⁸ Note that the optimized geometries agree quite well with experimental results, although both PW91 and OLYP overestimate the Fe–N_{imido} and Fe–P distances by about 0.02 Å. As shown in Figure 3, the optimizations confirm that the iron in Fe^{III}(PhBP^{iPr}₃)(NAd) exhibits close to exact C_{3v} local symmetry.³² Accordingly, we chose to examine the simplified C_{3v} complex Fe^{III}–(MeBP₃)(NMe) in some detail.

Figure 2(a,b) confirms that the electronic configuration of this complex may be described as $d_{xy}^2d_{x^2-y^2}^2d_{z^2}^1$ (or $d_{\delta}^2d_{\delta'}^2d_{\sigma}^1$). Note that the excess spin density is almost entirely on the Fe, with a small trace of cylindrically symmetric minority spin density on the imido nitrogen. This might suggest that the singly occupied molecular orbital (SOMO) is a pure d_{z^2} orbital, but it is not: it is about 50% Fe and 12% N_{imido}, interacting in an antibonding manner. The reason there is no majority spin on the imido nitrogen is that it is canceled by some of the excess minority spin left there by the spatial offset between the α - and β -spin Fe(d_{π})–N(p_{π}) π -bonding MOs.³³ The antibonding nature of the MO shown in Figure 2 implies an Fe–N_{imido} bond order of 2.5, that is, 0.5 σ bonds and 2 π bonds. However, there are two interesting twists to this picture.

First, note from Figure 2a that the Fe character of the SOMO is not simply due to a d_{z^2} contribution, but also to a significant p_z contribution. The Fe p_z contribution has the effect that the “top” lobe of the d_{z^2} orbital in Figure 2a is shrunken, while the “bottom” lobe is correspondingly swollen. We believe that this specific topology of the d_{z^2} orbital goes a long way toward minimizing the Fe–N_{imido} σ -antibonding interaction. Second, note that the top “green” lobe of the Fe d_{z^2} orbital is nearly enveloped by the equatorial “magenta” lobe (of the same orbital) as well as by the

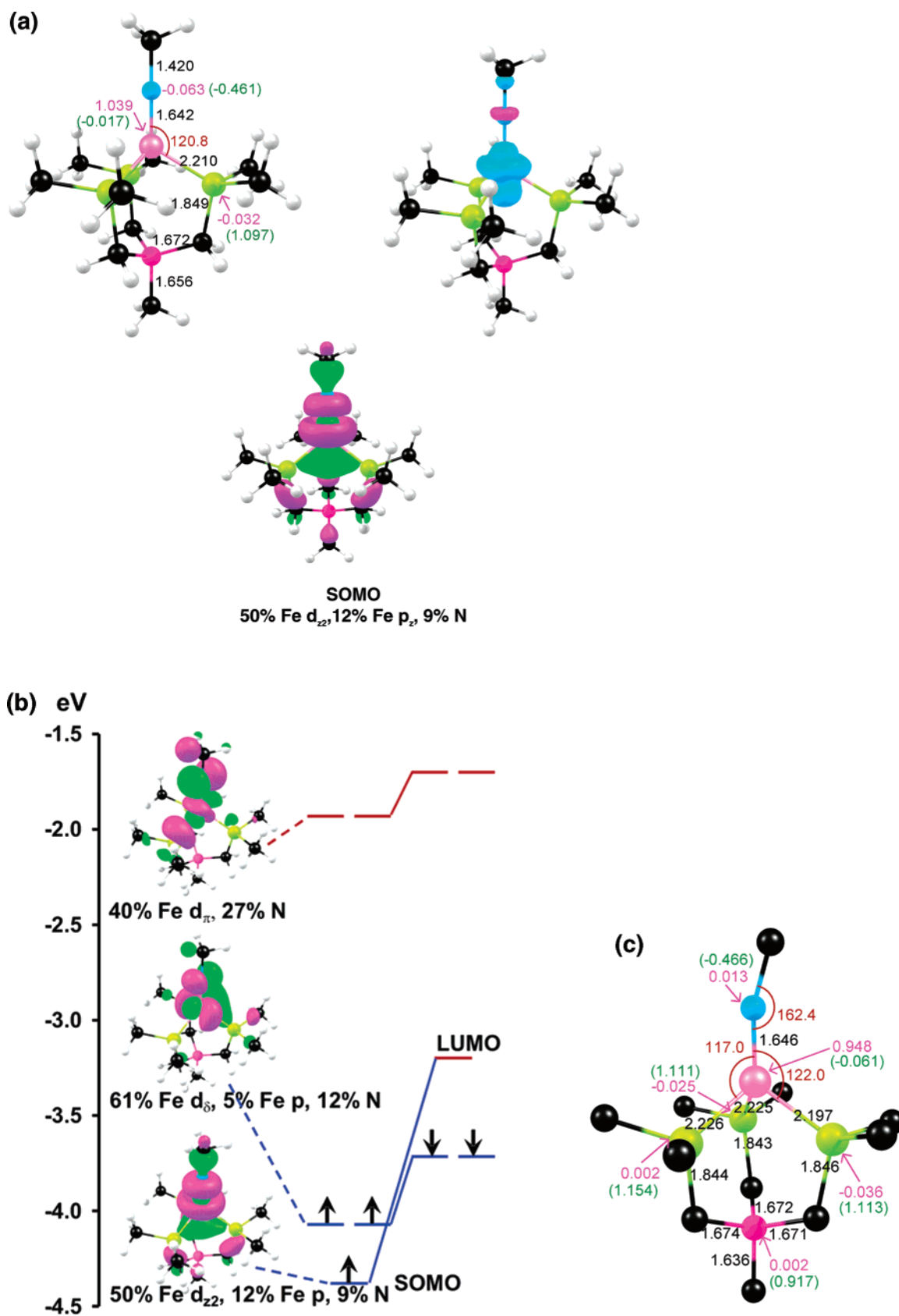


Figure 2. Selected results for $\text{Fe}^{\text{III}}(\text{MeBP}_3)(\text{NMe})$. (a) Results from a C_{3v} symmetry-constrained optimization. Top left: Optimized distances (\AA , in black), angles (deg, red), Mulliken spin populations (magenta), and charges (green, in parentheses); right: a plot of the spin density, with majority and minority spin densities indicated in cyan and magenta, respectively; bottom: a plot of the SOMO. (b) A C_{3v} valence MO energy-level diagram. (c) The symmetry-unconstrained optimized geometry, where the hydrogen atoms have been omitted for clarity.

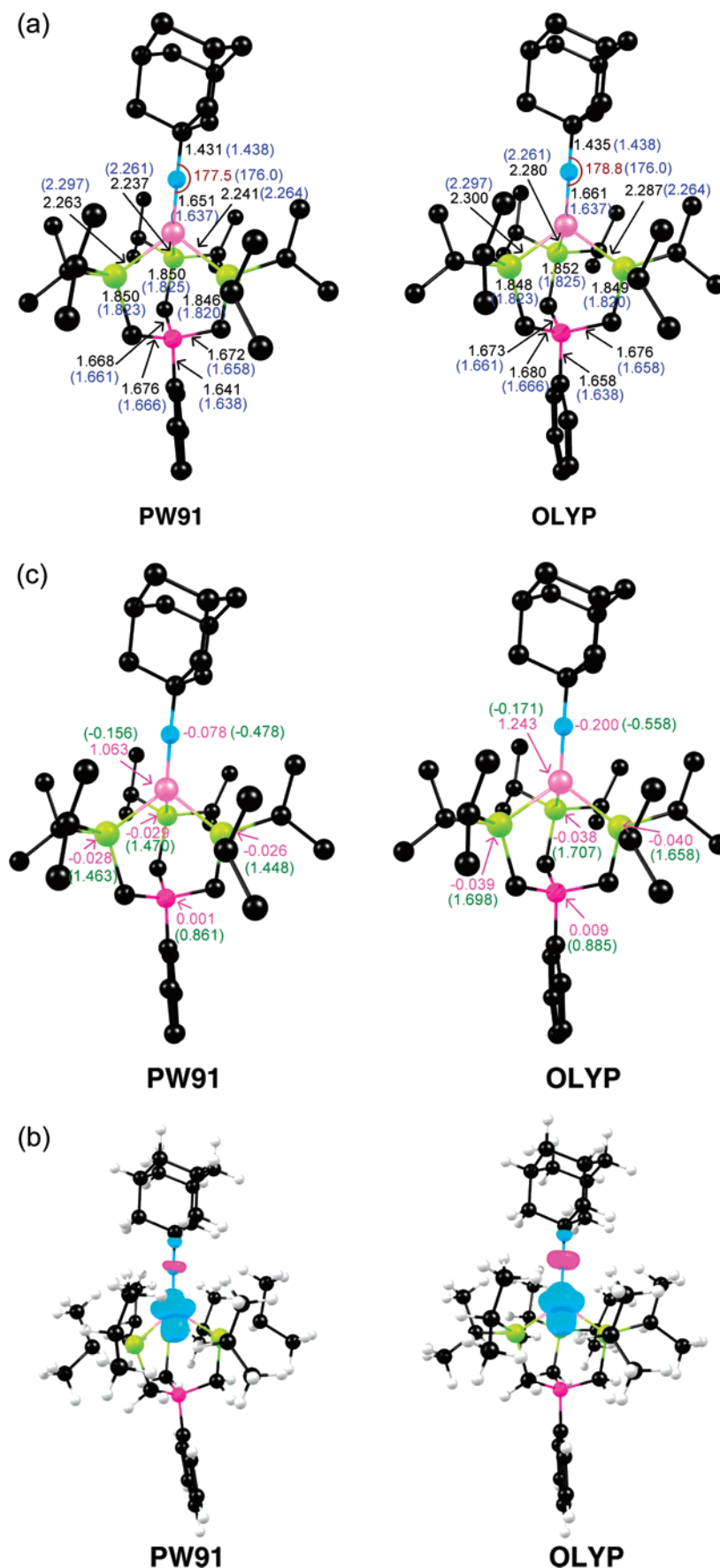


Figure 3. Selected PW91 and OLYP results from symmetry-unconstrained optimizations of $\text{Fe}^{\text{III}}(\text{PhBPiPr}_3)(\text{NAd})$, an actual molecule studied experimentally: (a) optimized distances (Å, in black), angles (deg, in red), experimental values (blue); (b) Mulliken charges (green) and spin populations (magenta); and (c) spin density profiles. For clarity, hydrogen atoms have been omitted from parts a and b.

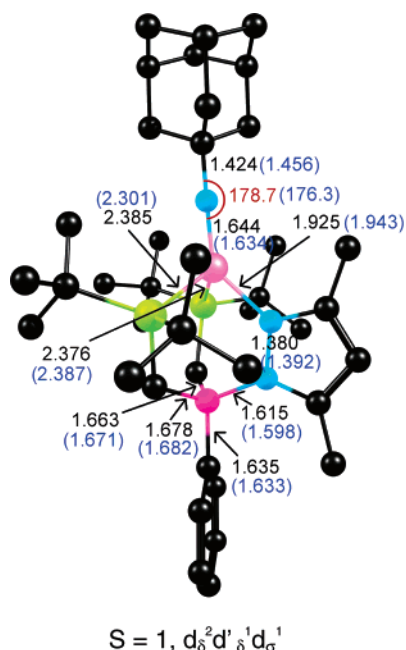


Figure 4. Selected PW91 results for $[\text{Fe}^{\text{IV}}(\text{PhBP}^{\text{Me}_2}\text{pz})(\text{NAd})]^+$, the actual molecule studied experimentally: optimized distances (Å, in black), angles (deg, in red), and experimental values (blue). Hydrogen atoms have been omitted for clarity.

“magenta” lobe of the imido σ lone pair. This remarkable topology implies that the $\text{Fe}(d_z^2)-\text{N}(p_{\sigma})$ antibonding interaction is, in reality, not particularly destabilizing, which explains the occupancy of this orbital. Accordingly, the “real” FeN bond order is somewhat above the formal value of 2.5, though it is not quite 3, as it is in an $S = 0$ $\text{Fe}^{\text{IV}}\text{N}$ species (see discussion below).³⁴

Besides analyzing the bonding under C_{3v} symmetry, we also carried out a PW91 symmetry-unconstrained optimization of the model complex $\text{Fe}^{\text{III}}(\text{MeBP}_3)(\text{NMe})$. Key results from this calculation are shown in Figure 2c. Overall, neither the geometry nor the spin density profile change much on relaxation of the symmetry constraint, with one exception: the $\text{Fe}-\text{N}_{\text{imido}}-\text{C}$ angle, at 162.4° , is significantly more bent in $\text{Fe}^{\text{III}}(\text{MeBP}_3)(\text{NMe})$ than in the relatively sterically hindered complex $\text{Fe}^{\text{III}}(\text{PhBP}^{\text{Pr}_3})(\text{NAd})$ (see Figure 3).¹⁸ The MO energy-level diagram in Figure 2b readily suggests a reason for this bending. Thus, note the very close spacing of the d_{xy} and $d_{x^2-y^2}$ and d_{z^2} orbitals, implying that, under C_{3v} symmetry, the 2A_1 and 2E states should be very close in energy, setting the stage for a pseudo-Jahn–Teller distortion. Unfortunately, DFT being essentially a ground-state theory, we have not been able to separately converge this 2E state. Thus, quite intriguingly, the observed near-linearity of the imido linkage¹⁸ in $\text{Fe}^{\text{III}}(\text{PhBP}^{\text{Pr}_3})(\text{NAd})$ appears not to be an inherent feature of the $\text{Fe}^{\text{III}}-\text{imido}$ bonding, but rather a result of a pseudo-Jahn–Teller effect suppressed by ligand steric effects.

(b) $\text{Fe}^{\text{IV}}-\text{Imido}$ Complexes. Figure 4 compares optimized PW91 and experimental geometry parameters for $[\text{Fe}^{\text{IV}}(\text{PhBP}^{\text{Bu}_2}\text{pz})(\text{NAd})]^+$.¹⁹ Both the metal–ligand distances and the observed linearity of the imido linkage are well-reproduced in our calculations. However, to perform a more detailed analysis of the bonding, we chose a slightly

simplified C_s version of this molecule— $[\text{Fe}^{\text{IV}}(\text{PhBP}^{\text{Me}_2}\text{pz})(\text{NAd})]^+$ —for which key results are shown in Figure 5. Once again, the optimized metal–ligand distances in this molecule compare well with those experimentally observed for $[\text{Fe}^{\text{IV}}(\text{PhBP}^{\text{Bu}_2}\text{pz})(\text{NAd})]^+$, and the imido linkage is essentially linear.¹⁹ The latter strongly suggests a threefold-symmetric, Jahn–Teller-inactive electronic structure and, particularly for an $S = 1$ d^4 pseudotetrahedral metal ion, a $d_{xy}^1 d_{x^2-y^2}^1 d_{z^2}^2$ (or $d_{\delta}^1 d_{\delta'}^1 d_{\sigma}^2$) electronic configuration, as has indeed been proposed.¹⁹ However, our calculations indicate a somewhat different electronic configuration.

A plot of the spin density profile of $[\text{Fe}^{\text{IV}}(\text{PhBP}^{\text{Me}_2}\text{pz})(\text{NAd})]^+$, shown in Figure 5b, provided the first clues that the electronic configuration might not be as proposed. A $d_{xy}^1 d_{x^2-y^2}^1 d_{z^2}^2$ (or $d_{\delta}^1 d_{\delta'}^1 d_{\sigma}^2$) configuration should result in a cylindrically symmetric, flattened (oblate) spheroidal blob of spin density around the iron. Instead, the blob of spin density around the iron has a distinct six-lobed shape, which appears most consistent with an unpaired d_{δ} electron and an unpaired d_{z^2} electron. The MO energy-level diagram shown in Figure 5c confirms this picture: the d^4 electronic configuration is accounted for by a “doubly occupied” a' -symmetry d_{δ} -based MO, a singly occupied a'' -symmetry d_{δ} -based MO, and a singly occupied a' -symmetry d_{z^2} -based MO. The detailed views of the “open-shell MOs”, given in Figure 5d, may convey a clearer sense of the orbital interaction topologies. A somewhat subtle point concerns why the a' -symmetry d_{δ} MO is “doubly occupied” (i.e., both the α - and β -spin MOs of this type are occupied), while the a'' -symmetry d_{δ} MO is “singly occupied”. The answer is that the latter MO (shown in Figure 5d) is destabilized by relatively head-on antibonding interactions with two P atoms, whereas such antibonding interactions are essentially absent in the a' -symmetry d_{δ} -based MO.

Under C_{3v} symmetry, the above electronic configuration corresponds to a Jahn–Teller-active 3E state. Accordingly, we carried out a symmetry-unconstrained optimization of the sterically unhindered $S = 1$ $[\text{Fe}(\text{MeBP}_3)(\text{NMe})]^+$ complex, the results of which are shown in Figure 6. The FeNC angle (173°) is modestly bent, but more so than in $[\text{Fe}^{\text{IV}}(\text{PhBP}^{\text{Bu}_2}\text{pz})(\text{NAd})]^+$, the actual molecule studied experimentally.¹⁹ As in the case of $\text{Fe}^{\text{III}}-\text{imido}$ complexes, it appears that the sterically hindered ligands used experimentally effectively suppress the Jahn–Teller distortions that would otherwise be more pronounced. Careful examination of the optimized and crystallographic structures shows several short $\text{H}\cdots\text{H}$ contacts of around 2.5 Å in the NAd complexes, but none below 3.5 Å in the NMe model complexes.

(c) $\text{Fe}^{\text{IV}}-\text{Nitrido}$ Complexes. An $\text{Fe}^{\text{IV}}\text{N}$ trisphosphine species has also been reported and spectroscopically, but not structurally, characterized.³⁴ Accordingly, we modeled this species simply as $\text{Fe}^{\text{IV}}(\text{MeBP}_3)\text{N}$, the calculated PW91 results being shown in Figure 7a. Not surprisingly,³⁴ $\text{Fe}^{\text{IV}}(\text{MeBP}_3)\text{N}$ exhibits a C_{3v} $S = 0$ ground state, corresponding to a $d_{xy}^2 d_{x^2-y^2}^2$ (or $d_{\delta}^2 d_{\delta'}^2$) orbital occupancy. Note the extremely short FeN distance (1.52 Å), which is even slightly shorter than that observed for an octahedral $\text{Fe}^{\text{VI}}\text{N}$ complex (1.57),³⁵ reflecting the full triple-bond character of the FeN bond. Figure 7b shows that the orbital energy spacings in $\text{Fe}^{\text{IV}}-$

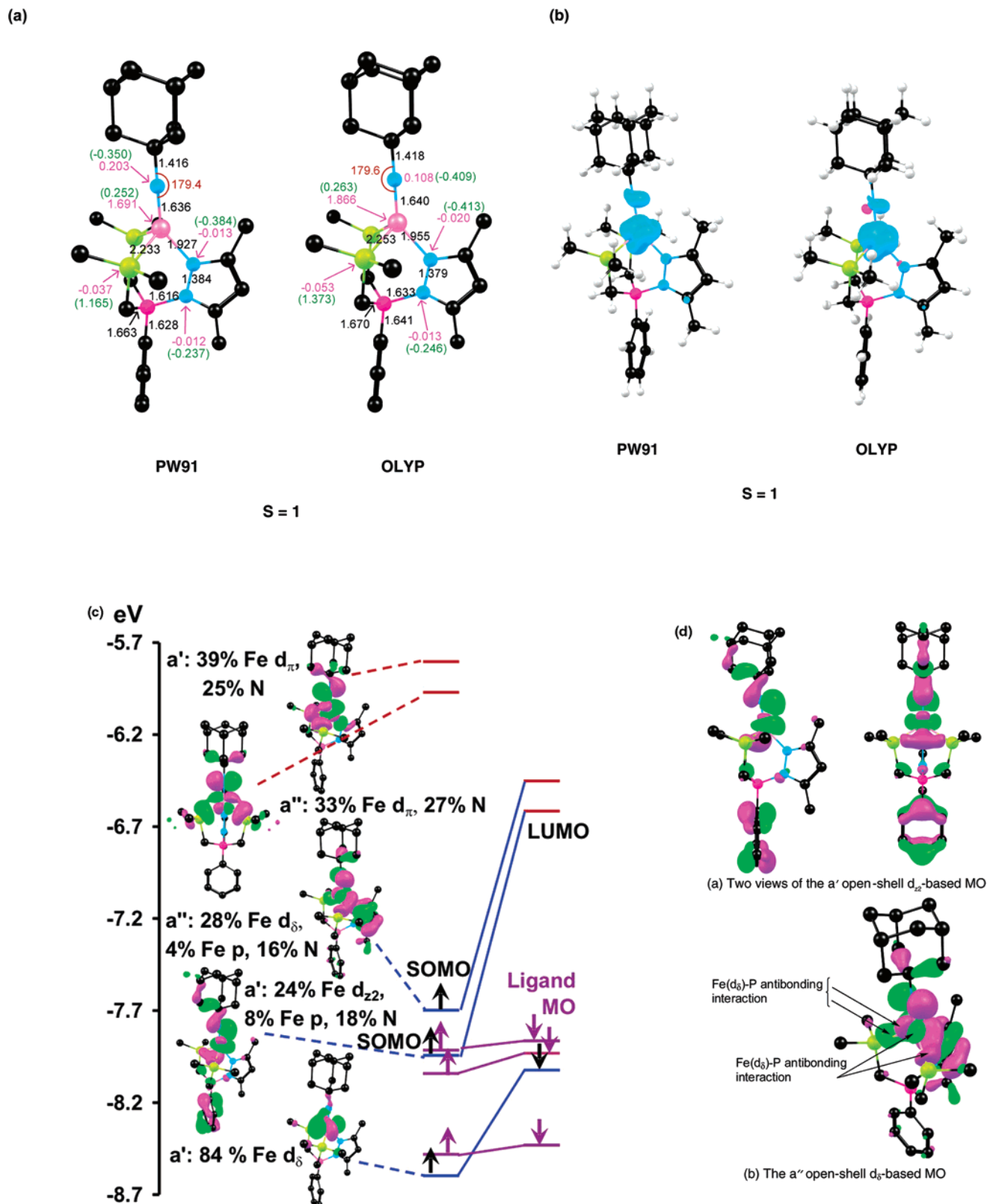


Figure 5. Selected PW91 and OLYP results for a C_s symmetry-constrained optimization of $[\text{Fe}^{\text{IV}}(\text{PhBP}^{\text{Me}}_2\text{pz})(\text{NAd})]^+$, which is a slightly simplified version of $[\text{Fe}^{\text{IV}}(\text{PhBP}^{\text{tBu}}_2\text{pz})(\text{NAd})]^+$, the actual species studied experimentally: (a) optimized distances (Å, in black), angles (deg, red), Mulliken spin populations (magenta), and charges (green, in parentheses); (b) plots of the spin density; (c) a spin-unrestricted valence MO energy-level diagram; and (d) detailed views of the two open-shell MOs. In part c, the atomic compositions of the five majority-spin d-based MOs are indicated in the same order, from top to bottom, as the corresponding MO pictures occur in the diagram. Hydrogen atoms have been omitted for clarity in parts a, c, and d.

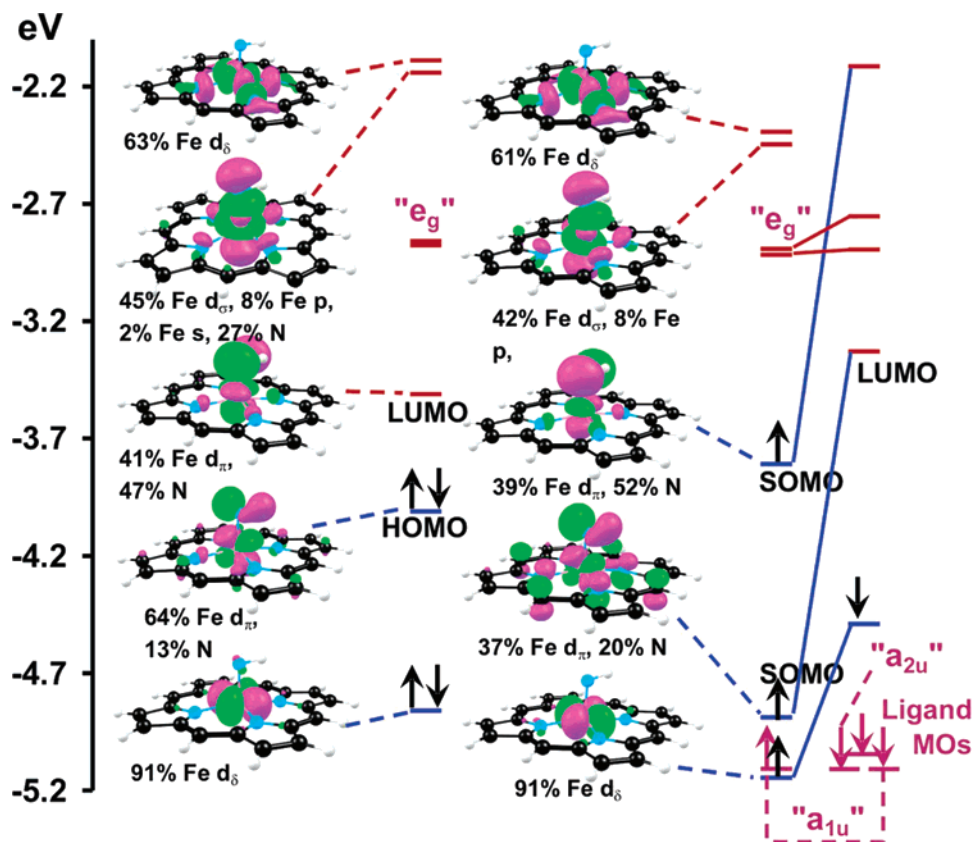


Figure 8. Frontier MO energy-level diagrams for the $S = 0$ (left) and 1 (right) states of $\text{Fe}^{\text{IV}}(\text{P})(\text{NH})$ (C_s). Selected porphyrin MOs are labeled in terms of standard D_{4h} irreps.

DFT calculations have shown that, in these trigonal-planar complexes, the “in-plane” d_{π} orbital (i.e., the one that is symmetric with respect to reflection across the MN_3 plane) is always of very high energy and is never occupied.^{24,36,37} This orbital is destabilized not only by the metal(d_{π})– $\text{N}_{\text{imido}}(\text{p}_{\pi})$ antibonding interactions but also by σ -antibonding interactions involving the β -diketiminato nitrogens. However, the other d_{π} orbital, the one antisymmetric with respect to the MN_3 plane, does not interact much with the β -diketiminato ligand and, therefore, is not prohibitively high in energy. Nevertheless, both d_{π} orbitals are higher in energy than the $d_{x^2-y^2}$ orbital, which points directly at the imido nitrogen, a situation similar to that of the d_z^2 orbital of the pseudotetrahedral complexes discussed above. These orbital spacing characteristics have the result that, while a β -diketiminato Co^{III} –imido complex avoids occupancy of *both* d_{π} orbitals and therefore has an $S = 0$ ground state,²⁴ an analogous Fe^{III} –imido complex only avoids the highest-energy d_{π} orbital and, therefore, adopts an $S = 3/2$ ground state.³⁸ In contrast, both $\text{Fe } d_{\pi}$ orbitals in the Fe^{III} –imido-phosphine complexes are high-energy unoccupied orbitals. Thus, the role of antibonding interactions involving the phosphine lone pairs in the destabilization of these d_{π} orbitals must not be underestimated.

Let us now return to what we view as an overarching theme of the metal–imido field, namely, that all structurally characterized middle and late transition-metal–imido complexes are low-coordinate, pseudotetrahedral, or trigonal-planar species. Iron–imido porphyrins remain unknown,¹⁵ even after decades of intense research on metalloporphyrin-

mediated catalytic processes. Indeed, to date, the sole example of an octahedral iron–imido species is a dicationic $S = 1$ Fe^{IV} –tosylimido intermediate, with a neutral polydentate N_5 supporting ligand. What accounts for the non-observation so far of Fe^{IV} –imido porphyrin intermediates? Is it *simply* that the appropriate experiments have not been attempted? We believe that the answer is “no”.

As alluded to above in a somewhat fragmentary fashion, low-coordinate stereochemistries facilitate metal–ligand multiple bonding involving middle and late transition metals in a number of ways. First, the lack of equatorial ligands in pseudotetrahedral and trigonal-planar metal–imido complexes results in a pair of very stable d_{δ} orbitals. Second, the absence of ligands both equatorial and trans to the imido group greatly stabilizes the d_z^2 orbital. Third, as mentioned above, the d_z^2 -based MO in imido complexes has a very special topology: the equatorial lobe of the d_z^2 orbital seems to curve up and engage in a *bonding* interaction with the imido lone pair, thereby significantly neutralizing the head-on antibonding interaction. More formally, this special shape may be described as significant p_z character mixing into the d_z^2 orbital. This results in an asymmetric d_z^2 orbital with a shrunken “top” lobe and a swollen “bottom” lobe. The lack of a ligand trans to the imido group in low-coordinate complexes implies that there are no antibonding interactions to destabilize the swollen bottom lobe of the d_z^2 orbital.

The bonding scenario in porphyrin and octahedral Fe^{IV} –imido species is radically different. The $d_{x^2-y^2}$ orbital, with its lobes pointing toward porphyrin nitrogens, is very high in energy. The equatorial “disk” of the d_z^2 orbital too

experiences strong antibonding interactions involving the porphyrin nitrogens. Only the d_{xy} orbital is relatively stable and free of substantial antibonding interactions. Accordingly, for an iron–imido porphyrin, the d_π orbitals, of necessity, have to be (at least partially) occupied. DFT calculations with a variety of functionals on the model complex $\text{Fe}^{\text{IV}}(\text{P})(\text{NH})$ predict nearly equienergetic $S = 0$ ($d_{xy}^2 d_{xz}^2$) and $S = 1$ ($d_{xy}^2 d_{xz}^1 d_{yz}^1$) states, with the latter very slightly lower in energy. The PW91 MO energy-level diagrams of these two states are shown in Figure 8. Of these two states, the $S = 0$ state in particular is expected to be highly susceptible to nucleophilic attack in view of its very low lying d_{yz} lowest unoccupied MO and a large amplitude on the imido nitrogen. Thus, even though an Fe^{IV} –imido porphyrin has an $S = 1$ ground state, the low-lying $S = 0$ state could easily provide the main channel for nucleophilic attack in processes such as aziridination, nitrene insertion, and so forth. On the other hand, triplet-state reactivity is more difficult to predict, on the basis of a MO diagram alone. However, overall, our calculations suggest that Fe^{IV} –imido porphyrins should be reactive species, considerably more so than the Fe–imido-phosphine complexes discussed above, at least in part as a result of the existence of a low-lying, electrophilic $S = 0$ state. From this point of view, Que et al.’s recent synthesis of an $S = 1$ Fe^{IV} –tosylimido species³⁹ illustrates an ingenious approach to synthesizing an octahedral iron–imido complex: presumably, the less basic tosylimido ligand destabilizes the d_π orbitals less than an alkyl- or arylimido group would. Nevertheless, the tosylimido intermediate was found to be more reactive than the analogous $\text{Fe}^{\text{IV}}\text{O}$ species, which may (or may not) be indicative of “two-state reactivity” involving a low-lying $S = 0$ state. Overall, the generation and detection of an Fe^{IV} –imido or –tosylimido porphyrin intermediate remains an exciting challenge for the future.

Conclusion

A thorough DFT analysis of pseudotetrahedral $\text{Fe}^{\text{III/IV}}$ –imido-phosphine complexes has yielded many detailed insights, the more important of which may be summarized as follows. The complexes studied feature surprisingly low-energy, singly or doubly occupied d_z^2 orbitals, where the z direction is identified with the Fe–N_{imido} axis. The low energy of this orbital appears to be due primarily to the low-coordinate nature of the complexes. The absence of equatorial ligands as well as of a ligand *trans* with respect to the imido ligand plays a key role in stabilizing the d_z^2 orbital as well as the complexes as a whole. Moreover, certain unique topological features of the d_z^2 -based MO ensure that the formally antibonding character of this MO is actually far less destabilizing than one might naively expect. In contrast, MO considerations suggest that iron–imido porphyrins should be substantially more reactive, at least in part because of the existence of a low-lying, electrophilic $S = 0$ state. Our DFT calculations also indicate a revised electronic description for the Fe^{IV} –imido complex, $[\text{Fe}^{\text{IV}}(\text{PhBP}^{\text{tBu}}\text{pz})(\text{NAd})]^+$.¹⁹ Thus, instead of a $d_{xy}^1 d_{xz}^2 d_{yz}^1 d_z^2$ (or $d_\delta^1 d_\sigma^1 d_z^2$) configuration, as originally proposed,¹⁹ our calculations indicate a $d_{xy}^2 d_{xz}^2 d_z^1$ (or $d_\delta^2 d_\sigma^1 d_z^1$) configuration. Geometry optimizations with simplified trisphosphine ligands (such as MeBP_3) indicate

that the observed linearity of the imido linkages might not be an inherent, electronically dictated phenomenon. Thus, both $\text{Fe}^{\text{III}}(\text{MeBP}_3)(\text{NMe})$ and $[\text{Fe}^{\text{IV}}(\text{MeBP}_3)(\text{NMe})]^+$ exhibit distinctly (albeit modestly) bent FeNC angles, 162.4° and 173.1°, respectively, which we have attributed to pseudo-Jahn–Teller and Jahn–Teller distortions, respectively. Apparently, these distortions are not seen in the experimentally studied complexes because of the sterically hindered nature of the ligands employed.^{16–19} Nevertheless, the electronic near-degeneracies responsible for the bent imido units in the MeBP_3 complexes are important aspects of the electronic structures of pseudotetrahedral iron–imido complexes, which we should not lose sight of.

Acknowledgment. This work was supported by the Research Council of Norway, the South African National Research Foundation (grant number 2067416), and the Central Research Fund of the University of the Free State.

Supporting Information Available: Optimized Cartesian coordinates (25 pages) for the various complexes studied. This information is available free of charge via the Internet at <http://pubs.acs.org>.

References

- (1) Holm, R. H. *Chem. Rev.* **1987**, 97, 1401–1449.
- (2) Shan, X. P.; Que, L., Jr. *J. Inorg. Biochem.* **2006**, 100, 421–433.
- (3) Wigley, D. E. *Prog. Inorg. Chem.* **1994**, 42, 239–482.
- (4) Mehn, M. P.; Peters, J. C. *J. Inorg. Biochem.* **2006**, 100, 634–643. See also references herein for citations to the earlier literature in this field.
- (5) Mayer, J. M. *Comments Inorg. Chem.* **1988**, 8, 125–135.
- (6) Nugent, W. A.; Mayer, J. M. *Metal–Ligand Multiple Bonds*; Wiley: New York, 1998.
- (7) Groves, J. T. *J. Inorg. Biochem.* **2006**, 100, 434–447.
- (8) Harris, D. L. *Curr. Opin. Chem. Biol.* **2001**, 100, 724–735.
- (9) Czernuszewicz, R. S.; Su, Y. O.; Stern, M. K.; Macor, K. A.; Kim, D.; Groves, J. T.; Spiro, T. G. *J. Am. Chem. Soc.* **1988**, 110, 4158–4165.
- (10) Ghosh, A.; Gonzalez, E. *Isr. J. Chem.* **2000**, 40, 1–8.
- (11) Nakamoto, K. *Coord. Chem. Rev.* **2002**, 226, 153–165.
- (12) Dey, A.; Ghosh, A. *J. Am. Chem. Soc.* **2002**, 124, 3206–3207.
- (13) Harischandra, D. N.; Zhang, R.; Newcomb, M. *J. Am. Chem. Soc.* **2005**, 127, 13776–13777.
- (14) Wasbotten, I. H.; Ghosh, A. *Inorg. Chem.* **2006**, 45, 4910–4913.
- (15) An $S = 0$ Fe^{IV} –aminoimido or Fe^{II} –aminonitrene porphyrin has been reported. However, we do not view this as a simple Fe^{IV} –imido porphyrin, but rather as an Fe^{II} –diazoalkane complex, as we hope to describe in detail in a forthcoming paper. See: Mahy, J.-P.; Battioni, P.; Mansuy, D.; Fisher, J.; Weiss, R.; Mispelter, J.; Morgenstern-Badarau, I.; Gans, P. *J. Am. Chem. Soc.* **1984**, 106, 1699–1706.
- (16) Brown, S. D.; Betley, T. A.; Peters, J. C. *J. Am. Chem. Soc.* **2003**, 125, 322–323.

- (17) Brown, S. D.; Peters, J. C. *J. Am. Chem. Soc.* **2005**, *127*, 1913–1923.
- (18) Betley, T. A.; Peters, J. C. *J. Am. Chem. Soc.* **2003**, *125*, 10782–10783.
- (19) Thomas, C. M.; Mankad, N. P.; Peters, J. C. *J. Am. Chem. Soc.* **2006**, *128*, 4956–4957.
- (20) Jenkins, D. M.; Betley, T. A.; Peters, J. C. *J. Am. Chem. Soc.* **2002**, *124*, 11238–11239.
- (21) Hu, X.; Meyer, K. *J. Am. Chem. Soc.* **2004**, *126*, 16322–16323.
- (22) Shay, D. T.; Yap, G. P. A.; Zakharov, L. N.; Rheingold, A. L.; Theopold, K. H. *Angew. Chem., Int. Ed.* **2005**, *44*, 1508–1510.
- (23) The $S = 1$ ground state reported in ref 22 is in error. The ground state is $S = 0$, and the $S = 1$ state is a low-lying excited state. Corrigendum: Shay, D. T.; Yap, G. P. A.; Zakharov, L. N.; Rheingold, A. L.; Theopold, K. H. *Angew. Chem., Int. Ed.* **2006**, *45*, 7870–7870. We thank Professor Theopold for helpful discussions on this issue.
- (24) Dai, X.; Kapoor, P.; Warren, T. H. *J. Am. Chem. Soc.* **2004**, *126*, 4798–4799.
- (25) Perdew, J. P.; Chevary, J. A.; Vosko, S. H.; Jackson, K. A.; Perderson, M. R.; Singh, D. J.; Fiolhais, C. *Phys. Rev. B.: Condens. Matter Mater. Phys.* **1992**, *46*, 6671–6687.
- (26) Velde, G. T.; Bickelhaupt, F. M.; Baerends, E. J.; Guerra, C. F.; Van Gisbergen, S. J. A.; Snijders, J. G.; Ziegler, T. J. *J. Comput. Chem.* **2001**, *22*, 931–967.
- (27) Handy, N. C.; Cohen, A. *J. Mol. Phys.* **2001**, *99*, 403–412.
- (28) Ghosh, A. *J. Biol. Inorg. Chem.* **2006**, *11*, 671–673.
- (29) Ghosh, A. *J. Biol. Inorg. Chem.* **2006**, *11*, 712–724.
- (30) Roos, B. O. *Acc. Chem. Res.* **1999**, *32*, 137–144.
- (31) Ghosh, A.; Taylor, P. R. *Curr. Opin. Chem. Biol.* **2003**, *91*, 113–124.
- (32) For a definition of the local symmetry group, see: Mislow, K.; Siegel, J. *J. Am. Chem. Soc.* **1984**, *106*, 3319–3328.
- (33) Such spatially offset π -bonding interactions are well-precedented. See, e.g., Figure 4 and the related discussion on minority spin density on the NO group in $S = 1/2$ (d_{xy}^1) Mo(P)(NO)–(CH₃OH) (P = porphyrin) in: Tangen, E.; Ghosh, A. *J. Inorg. Biochem.* **2005**, *99*, 959–962.
- (34) Betley, T. A.; Peters, J. C. *J. Am. Chem. Soc.* **2004**, *126*, 6252–6254.
- (35) Berry, J. F.; Bill, E.; Bothe, E.; George, S. D.; Mienert, B.; Neese, F.; Wieghardt, K. *Science* **2006**, *312*, 1937–1941.
- (36) Holland, P. L.; Cundari, T. R.; Perez, L. L.; Eckert, N. A.; Lachicotte, R. J. *J. Am. Chem. Soc.* **2002**, *124*, 14416–14424. Addition/Correction: *J. Am. Chem. Soc.* **2003**, *125*, 11772–11772.
- (37) Kogut, E.; Wiencko, H. L.; Zhang, L. B.; Cordeau, D. E.; Warren, T. H. *J. Am. Chem. Soc.* **2005**, *127*, 11248–11249.
- (38) Eckert, N. A.; Vaddadi, S.; Stoian, S.; Lachicotte, R. J.; Cundari, T. R.; Holland, P. L. *Angew. Chem., Int. Ed.* **2006**, *45*, 6868–6871.
- (39) Klinker, E. J.; Jackson, T. A.; Jensen, M. P.; Stubna, A.; Juhasz, G.; Bominaar, E. L.; Münck, E.; Que, L., Jr. *Angew. Chem., Int. Ed.* **2006**, *45*, 7394–7397.

CT600318N